Supplementary Information for

A Top-Down Methodology for Ultrafast Tuning of Nanosized Zeolites

1. Experimental Section

Post-synthesis milling of zeolites: Post-synthesis milling was conducted on a bead milling apparatus (LMZ015, Ashizawa Finetech Ltd., Japan) using ZrO_2 as beads (size of the beads: 300 μm). Typically, 10 g of zeolites was dispersed in 50 g pure water to get a slurry. This slurry was then fed by a gear pump into the milling chamber, where the beads were rotating at a rate of 3000 rpm. After a certain milling period, the milled slurry was collected and dried to obtain the millled zeolites.

Preparation of the supernatant liquid: The supernatant liquid used for the recrystallization was collected from the synthesis of the raw zeolites rather than specifically prepared. After the fast synthesis, centrifugation was performed to separate solid and liquid phases. The solid phase was further washed and dried to obtain the raw zeolites, whereas the liquid phase was kept for the recrystallization without any further treatment. The supernatant liquid may contain trace amount of residual species, such as OSDA and Si. The chemical composition of the supernatant liquid has not yet been quantitatively measured.

Procedure of the fast recrystallization: The milled zeolites were mixed into the supernatant liquid to get a synthesis gel. Typically, 1.5 ml of the synthesis gel was transferred to the tubular reactor and sealed upon which the reactor was immersed in a preheated oil bath (210 ^{o}C for SSZ-13 and 190 ^{o}C for $AlPO_4$-5). After a specific hydrothermal treatment time the tubular reactor was quenched in cooling water. The reactant inside the reactor was downloaded, washed, centrifuged and dried to obtain the recrystallized zeolites.

Continuous-flow recrystallization of SSZ-13: A stainless steel tube with inner/outer diameters of 4.4/6.4 mm was used as the continuous flow reactor. A high pressure syringe pump (Micro Feeder JP-H, Furue Science, Japan) was used to feed the synthesis gel (same as described in *Procedure of the fast recrystallization*). The length of the flow reactor immersed within the silicon oil bath was 15 cm to ensure a residence time of 10 min. Pure water was supplied by a HPLC pump (MP311, Lab-Quatec, Japan) to dilute and cool the fluid flowing out of the oil bath. The system pressure was controlled by a back pressure regulator (TESCOM 26-1700, Emerson, US) installed before the outlet of the continuous flow reactor.[1,2] The pressures at both ends of the flow reactor were measured using two pressure gauges, and the pressure was recorded by a home-made digital recorder. A safety valve and an alarm system were installed for safety considerations.

Characterizations: Powder X-ray diffraction (XRD) patterns of the samples (as-synthesized, unless otherwise sepcified) were collected on a Rigaku Ultima IV diffractometer

using CuKα radiation (λ=0.15406 nm, 40 KV, 40 mA) at a scanning rate of 4 °/min. Raman spectra were recorded on a laser Raman spectrometer (JASCO Corp., NRS-1000) using an argon green laser at a wavelength of 532 nm for excitation. The morphology of the products was observed by FE-SEM (JSM-7000F, JEOL, Japan) with an accelerating voltage at 15 keV. TEM observations were carried out using a JEM 2010 transmission electron microscope (JEOL, Japan) operated at 200 keV. Before the observations, the samples were sputter-coated with Os. Solid-state magic-angle spinning nuclear magnetic resonance (MAS NMR) spectra were collected by a JEOL ECA 500 spectrometer. Nitrogen adsorption-desorption measurements of the calcined samples were performed on the Autosorb-1 instrument (Quantachrome Instruments) at 77 K. Before the measurements, the samples were pretreated at 400 °C for 6 h under vacuum. High-energy X-ray Total Scattering (HEXTS) measurements were performed on powder sample in a quartz capillary at room temperature using a horizontal two-axis diffractometer at the BL04B2 high-energy X-ray diffractionbeamline (SPring-8, Japan). The energy of incident X-rays was 61.43 keV (λ = 0.2018 Å). The maximum Q ($Q = 4\pi\sin\theta/\lambda$), Q_{max}, collected in this study was 25 Å^{-1}. The obtained data were subjected to well-established analysis procedures, such as absorption, background, and Compton scattering corrections, and subsequently normalized to give a Faber–Ziman total structure factor $S(Q)$[3,4]. These collected data were used to calculate the pair distribution function,$G(r)$, using the following function:

$$G(r) = 4\pi r[\rho(r) - \rho_0] = \frac{2}{\pi}\int_{Qmin}^{Qmax} Q[S(Q) - 1]\sin(Qr)dQ,$$

where ρ is the atomic number density (for example, 0.0531/Å^3 for Na: 1, Al: 1, Si: 12, O: 26, 2.0 g/cm^3).

References:

[1] Z. Liu, T. Wakihara, K. Oshima, D. Nishioka, Y. Hotta, S. P. Elangovan, Y. Yanaba, T. Yoshikawa, W. Chaikittisilp, T. Matsuo, T. Takewaki, T. Okubo, *Angew. Chem. Int. Ed.* **2014**, 54, in press.

[2] Z. Liu, T. Wakihara, D. Nishioka, K. Oshima, T. Takewaki, T. Okubo, *Chem. Mater.* **2014**, 26, 2327-2331.

[3] T. E. Faber, J. M. Ziman, *Philos. Mag.* **1965**, 11, 153–173.

[4] S. Kohara, M. Itou, K. Suzuya, Y. Inamura, Y. Sakurai, Y. Ohishi, M. Takata, *J. Phys. Condens. Matter* **2007**, 19, 506101.

2. Supplementary Figures

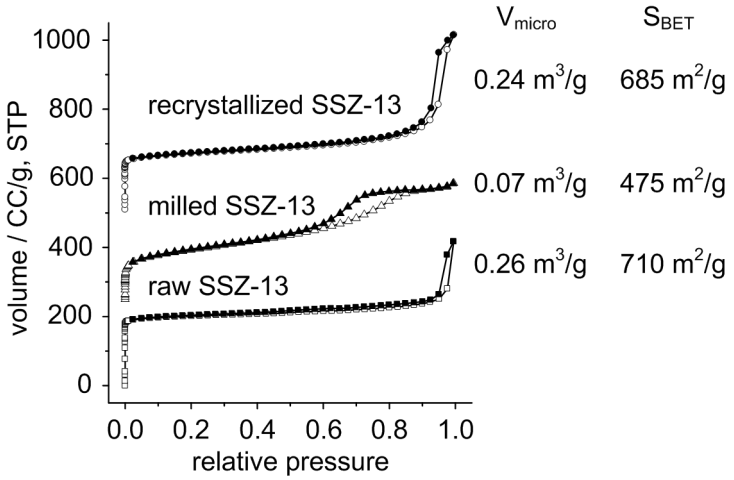

Figure S1 BET isotherms of (a) raw SSZ-13, (b) milled SSZ-13 (milled for 60 min) and (c) nano-sized SSZ-13 (recrystallized for 10 min in the tubular reactor). (Offset for each entry in *y*-axis: 250).

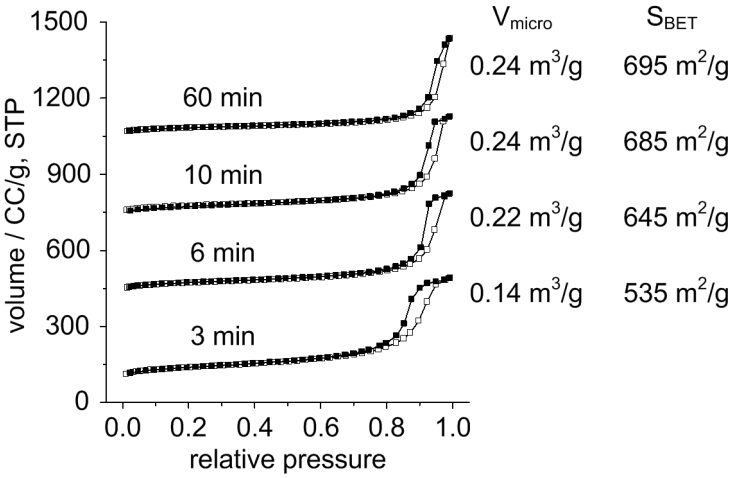

Figure S2 BET isotherms of the recrystallized SSZ-13 samples with different recrystallization times. (Offset for each entry in *y*-axis: 300).

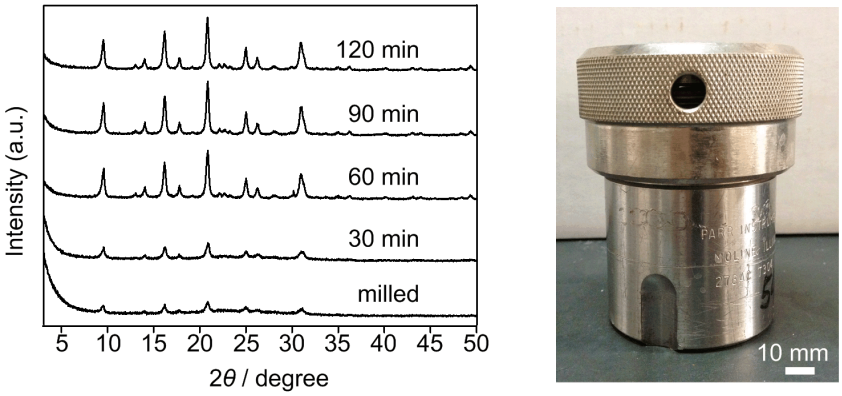

Figure S3 Recrystallization in the conventional autoclave: milled SSZ-13 and the samples recrystallized in autoclave for 30 min, 60 min, 90 min and 120 min, respectively. Photograph of the autoclave (Parr, #4749) is shown in the right.

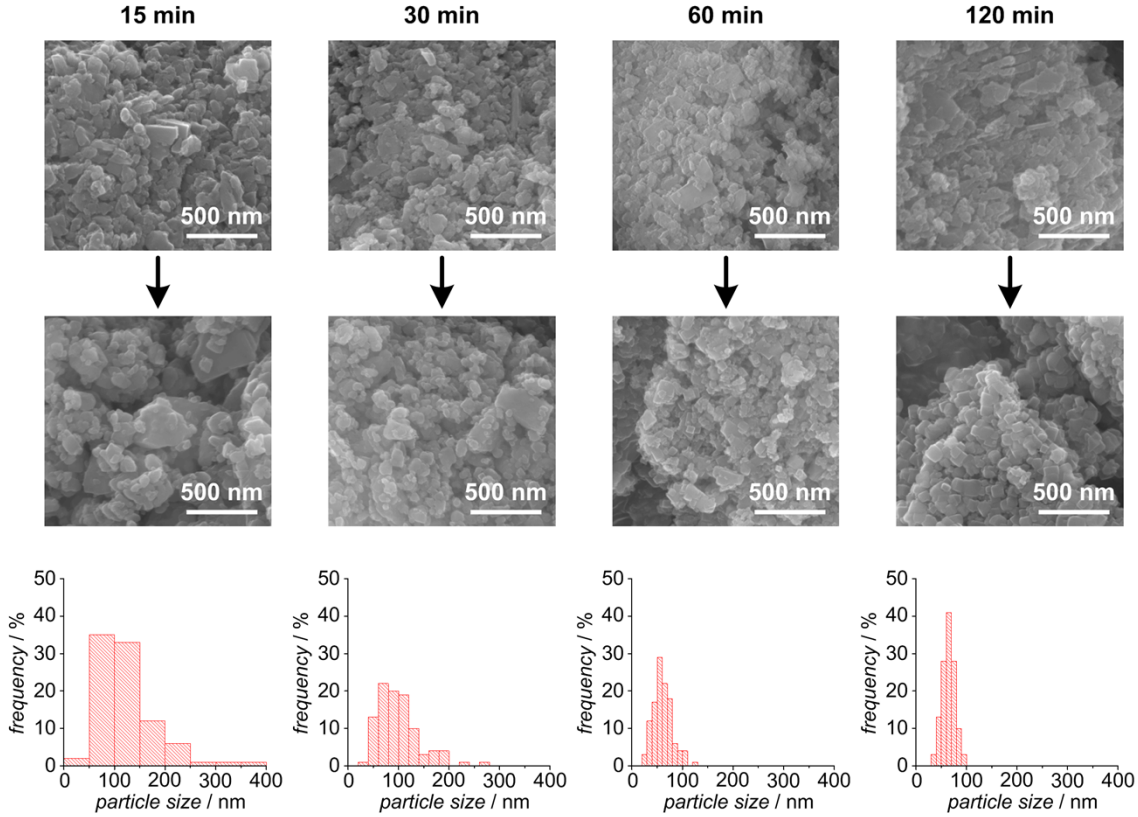

Figure S4 Effect of milling time on particle size of recrystallized SSZ-13. The upper row shows the milled SSZ-13 with different milling time, the middle row shows the recrystallized SSZ-13, and the lower row shows the particle size distribution of the recrystallized products. (Recrystallization time: 10 min).

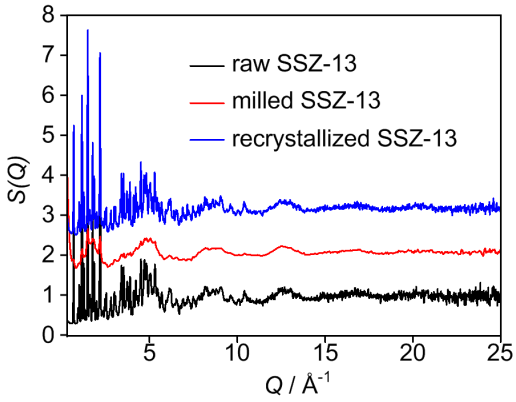

Figure S5 Total structure factors, *S(Q)*, of raw SSZ-13, milled SSZ-13 and recrystallized SSZ-13

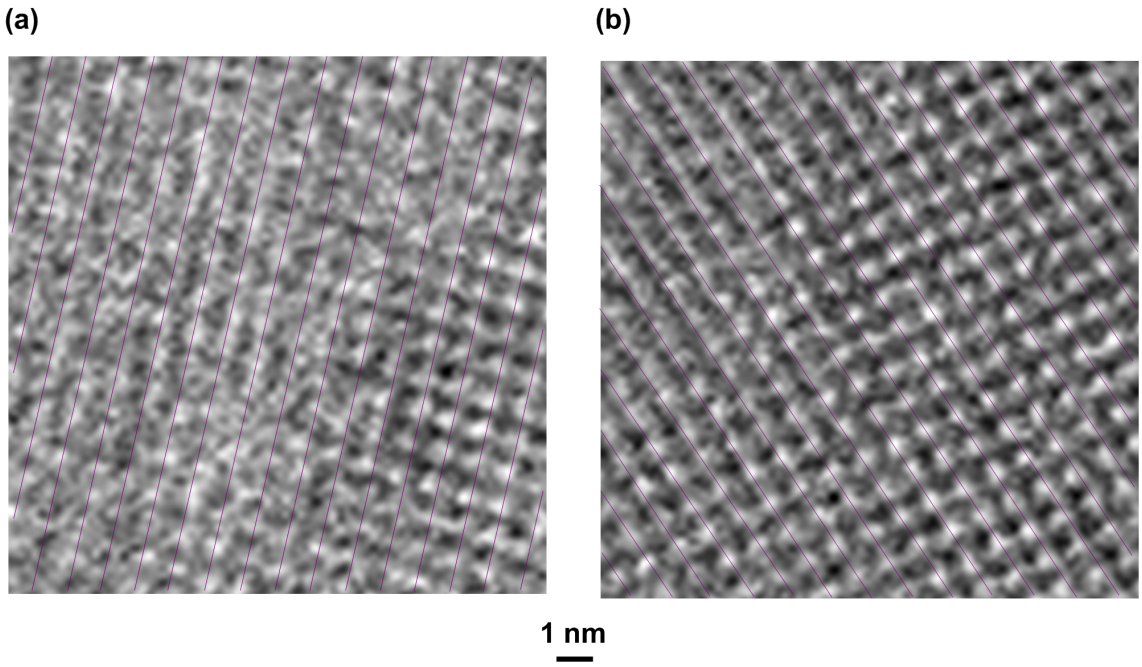

Figure S6 Magnified TEM photos with grids to show the distortion of the milled SSZ-13: (a) milled SSZ-13; (b) recrystallized SSZ-13. (The grids help to identify the distorted lattice of the milled SSZ-13. As clearly showed, some lattice dots for the milled SSZ-13 are not following the guiding grids, indicating of distortion of the lattice. In contrast, the lattice dots are well under the grids, demonstrating that the crystalline connectivity was restored).

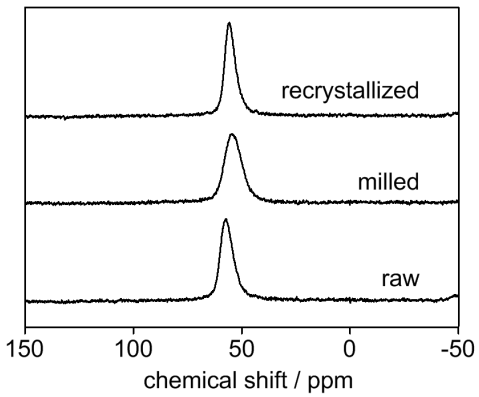

Figure S7 ^{27}Al solid NMR spectra of raw SSZ-13, milled SSZ-13 and recrystallized SSZ-13.

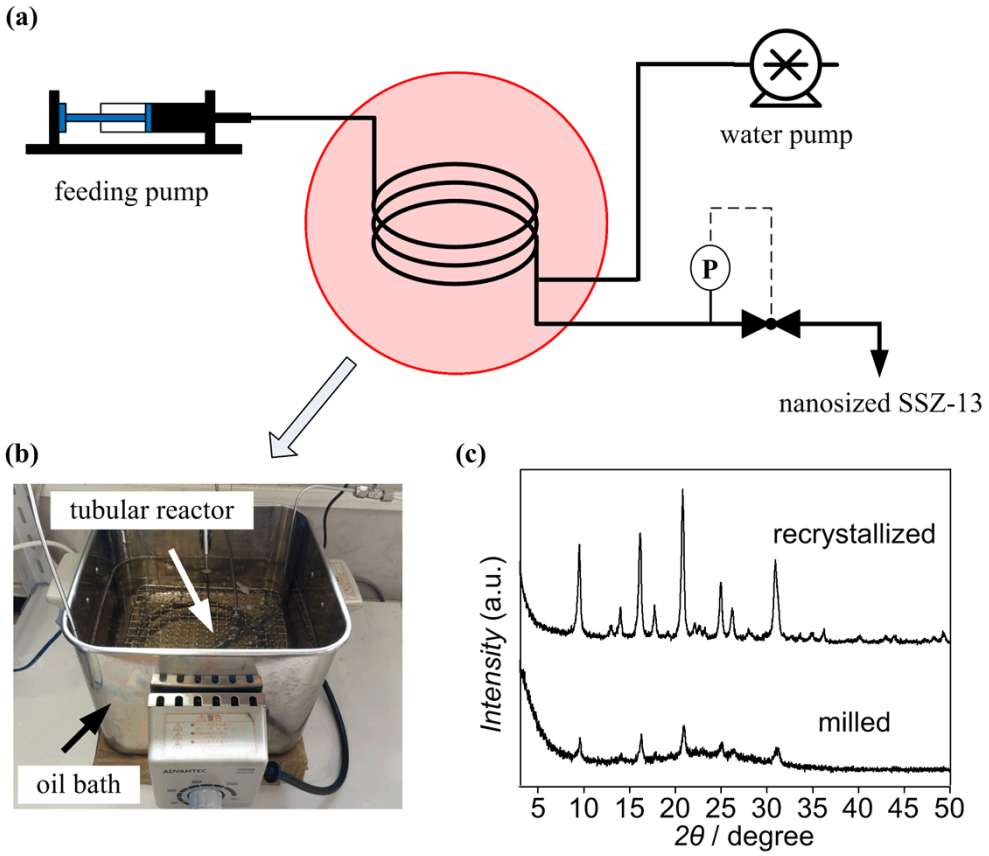

Figure S8 Continuous flow recrystallization of SSZ-13. (a) Flow diagram for the continuous flow recrystallization. (b) Illustration of the tubular reactor in the oil bath. (c) XRD patterns for the recrystallized SSZ-13 obtained in the continuous flow reactor and the milled SSZ-13.

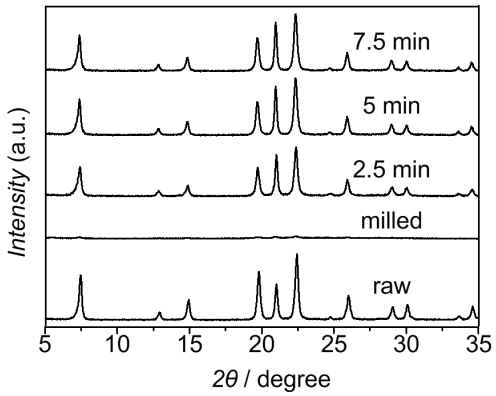

Figure S9 XRD patterns for $AlPO_4$-5 samples, including raw $AlPO_4$-5, milled $AlPO_4$-5 and recrystallized $AlPO_4$-5 samples with different recrystallization in the tubular reactor.